Editors' Suggestion

Homogenization Theory of Space-Time Metamaterials

P.A. Huidobro,[1,*] M.G. Silveirinha,[1] E. Galiffi,[2] and J.B. Pendry[2]

[1] *Instituto de Telecomunicações, Instituto Superior Tecnico—University of Lisbon, Avenida Rovisco Pais 1, Lisboa 1049-001, Portugal*

[2] *The Blackett Laboratory, Department of Physics, Imperial College London, London SW7 2AZ, United Kingdom*

(Received 22 September 2020; revised 20 June 2021; accepted 24 June 2021; published 19 July 2021)

We present a general framework for the homogenization theory of space-time metamaterials. By mapping to a frame comoving with the space-time modulation, we derive analytical formulas for the effective material parameters for traveling-wave modulations in the low-frequency limit: electric permittivity, magnetic permeability, and magnetoelectric coupling. In doing so, we provide a recipe for the calculation of effective parameters of space–time-modulated media where the parameters follow a traveling-wave form of any shape and we show how synthetic motion can result in giant bianisotropy. This allows us to deepen the understanding of how nonreciprocity can be achieved in the long-wavelength limit and to completely characterize the different nonreciprocal behaviors available in space–time-modulated media. In particular, we show how the modulation speed, which can be subluminal or superluminal, together with the relative phase between electric and magnetic modulations, provide tuning knobs for the nonreciprocal response of these systems. Furthermore, we apply the theory to derive exact formulas for the Fresnel drag experienced by light traveling through traveling-wave modulations of electromagnetic media, providing insight into the differences and similarities between synthetic motion and moving matter. Since we exploit a series of Galilean coordinate transformations, the theory may be generalized to other kinds of waves.

DOI: 10.1103/PhysRevApplied.16.014044

I. INTRODUCTION

Enabled by the advent of new materials and techniques to achieve fast and efficient dynamical modulation of material parameters [1–3], the emergence of time as a new degree of freedom for the design of metamaterials has recently opened different and intriguing avenues for wave control [4]. Modulations of a material parameter in time, as well as in space, enable frequency-momentum transitions [3,5], nonreciprocal effects [6–13], compact photonic isolators and circulators without magnetic bias [14–16], harmonic generation [17], unidirectional amplification [18], topological phases [19–22], and multifunctional nonreciprocal metasurfaces [23].

Periodic space-time modulations of the permittivity and permeability in space and time following a traveling-wave form,

$$\epsilon(x,t) = \epsilon(x - vt), \quad \mu(x,t) = \mu(x - vt), \tag{1}$$

have attracted much attention since early research [24–26]. In these expressions, v denotes the modulation speed, which, since we are concerned with modulations and not with moving media, is not bounded by the speed of light. Figure 1(a) shows a sketch of a sinusoidal space-time modulation. The spatial, g, and temporal, Ω, modulation frequencies determine the modulation speed as $v = \Omega/g$. Traveling-wave modulations impose a linear-momentum bias, breaking time-reversal symmetry and resulting in nonsymmetric high-frequency band gaps, which can be exploited for frequency-momentum transitions and nonreciprocal devices [see Fig. 1(b)] [3,8]. Recently, it has been shown that the need for working at high frequencies (near the band gap) can be lifted and nonreciprocity emerges as a linear broadband phenomenon in *luminal* modulations of the permittivity [see Fig. 1(c)]. Space-time modulations at speeds approaching those of waves in a medium result in nonreciprocal broadband amplification [18]. Interestingly, nonreciprocity can be achieved in the long-wavelength limit and even at zero frequency if both electromagnetic parameters, ϵ and μ, are modulated [10] [see Figs. 1(e) and 1(f)], realizing a synthetic tunable form of Fresnel drag [12].

Despite the broad interest raised by space-time media, most of the theoretical tools employed for their analysis are based on semianalytical or numerical approaches, such as Floquet-Bloch theory [25,26], transfer-matrix theory [27], finite-element methods [28], or perturbative Floquet-Bloch approaches [11,12]. On the other hand, the field of metamaterials has been fueled by a powerful technique: the homogenization of material response, which allows us to accurately describe a medium through effective material

*p.arroyo-huidobro@lx.it.pt

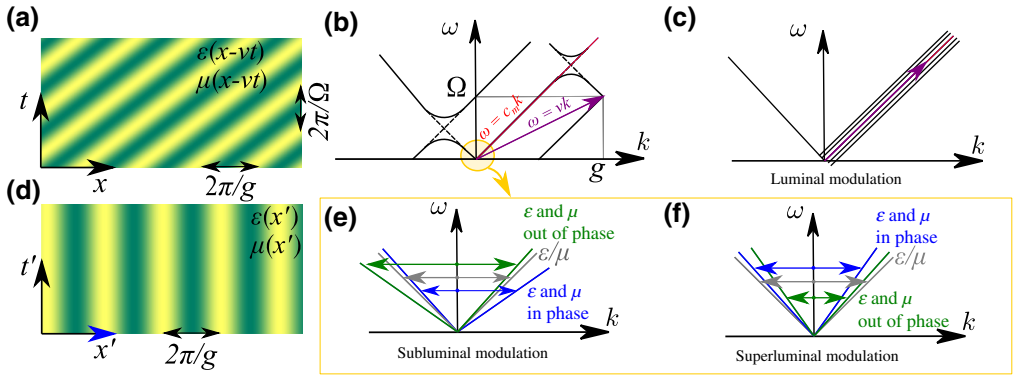

FIG. 1. Synthetic motion in space–time-modulated metamaterials enables nonreciprocity in the effective-medium limit. (a),(d) Traveling-wave modulations of the electromagnetic parameters as seen from the laboratory frame (a, unprimed coordinates) and from a frame comoving with the modulations (d, primed coordinates). (b) A sketch of a representative band diagram of space–time-modulated media: the bands are displaced by the space-time reciprocal lattice vector (g, Ω). Nonsymmetric band gaps open in non-impedance matched systems, such as with space-time modulations of only the permittivity. (c) Homogenization breaks down for modulation speeds approaching the speed of waves in the medium: the luminal regime is characterized by nonreciprocal wave amplification at any frequency. (e),(f) In the long-wavelength limit, the response is nonreciprocal only if both the permittivity and the permeability are modulated in space and time. The modulation speed and the phase between the electric and magnetic modulations are the knobs for tuning the nonreciprocal response through the interplay between effective permittivity, effective permeability, and effective magnetoelectric coupling.

parameters in the long-wavelength limit. Here, we present a homogenization framework of space-time electromagnetic metamaterials. By transforming Maxwell's equations to the frame comoving with the modulation [see Fig. 1(d)], we analytically derive closed-form expressions to calculate the effective electromagnetic parameters of space–time-modulated media. While related approaches have been employed to study stratified media in electromagnetics [29] and acoustics [30,31], here we show that the analytical formalism can be applied to stratified or sinusoidal traveling-wave modulations as long as a Bloch-wave picture is valid, enabling the identification and characterization of different regimes of nonreciprocity in space–time-modulated media. Additionally, we also propose an alternative approach to find the exact solution (without homogenization) of Maxwell's equations in space–time-modulated systems. Specifically, working in the comoving frame where the time dependence of the material parameters disappears, we show that the electrodynamics can be characterized using the same long-established methods that are commonly used to characterize standard time-invariant systems. This exact solution allows us to further validate our effective-medium description, proving that it is not approximate but exact for two cases: (i) at any frequency in the absence of back reflections (that is, if the system is impedance-matched) and (ii) in the metamaterial (long-wavelength) limit for the impedance-mismatched case.

This paper is structured as follows. We start by applying a Galilean coordinate transformation to Maxwell's equations with space–time-modulated parameters in Sec. II, which allows us to introduce a homogenization framework in the long-wavelength limit in Sec. III, as well as an exact theory when back reflections are not present in Sec. IV. Then, we exemplify our approach by calculating analytically the effective-medium parameters of traveling stratified media in Sec. V. Finally, in Sec. VI, we consider a sinusoidal traveling-wave modulation and derive analytical expressions for the effective-medium parameters and the Fresnel drag of light produced by this synthetic motion.

II. GALILEAN TRANSFORMATION OF MAXWELL'S EQUATIONS

The fields in space–time-modulated media satisfy Maxwell's equations,

$$\nabla \times \mathbf{E} = -\frac{\partial \mathbf{B}}{\partial t}, \quad \nabla \times \mathbf{H} = \frac{\partial \mathbf{D}}{\partial t}, \tag{2}$$

and are related through the constitutive equations as follows:

$$\mathbf{D}(x,y,z,t) = \epsilon(x - vt)\mathbf{E}(x,y,z,t), \tag{3}$$

$$\mathbf{B}(x,y,z,t) = \mu(x - vt)\mathbf{H}(x,y,z,t), \tag{4}$$

where ϵ and μ are deemed to include ϵ_0 and μ_0, respectively, which determine the speed of light in vacuum as $c_0 = 1/\sqrt{\epsilon_0\mu_0}$. We note that this represents the spatiotemporal modulation along one direction of otherwise isotropic but possibly inhomogeneous permittivity and permeability. Here, we assume that the system is not dispersive, although it is possible to generalize the theory

to include dispersion. We now give the key steps of our approach, while extensive derivations can be found in the Supplemental Material [32].

We start by considering a Galilean transformation to a comoving frame ($x' = x - vt$, $y' = y$, $z' = z$, $t' = t$). This is appropriate because we are dealing with parameter modulations, which can travel below, at, or above the speed of light. We have, for the parallel component of the fields,

$$\mathbf{D}'_{||} = \epsilon\left(x'\right)\mathbf{E}'_{||}, \quad \mathbf{B}'_{||} = \mu\left(x'\right)\mathbf{H}'_{||}, \tag{5}$$

where the primed fields depend on the transformed coordinates, (x', y', z', t'). The perpendicular components are transformed as

$$\begin{bmatrix}\mathbf{D}'_{\perp}\\ \mathbf{B}'_{\perp}\end{bmatrix} = \frac{1}{1-\epsilon(x')\mu(x')v^2} \times \begin{bmatrix}\epsilon(x')\mathbb{1} & -\epsilon(x')\mu(x')\mathbf{v}\times\mathbb{1}\\ \epsilon(x')\mu(x')\mathbf{v}\times\mathbb{1} & \mu(x')\mathbb{1}\end{bmatrix}\begin{bmatrix}\mathbf{E}'_{\perp}\\ \mathbf{H}'_{\perp}\end{bmatrix} \tag{6}$$

where $\mathbf{v}$ is the space-time modulation velocity vector and $\mathbb{1}$ is the 2×2 identity matrix. This shows that in the comoving frame, the modulation of parameters in space and time results in a moving-medium type coupling between the electric and magnetic fields. Conceptually, this implies that in the frame moving with the modulation, a bianisotropic coupling arises and the electromagnetic response is nonreciprocal. Interestingly, this is different from the usual moving-medium situation, where the bianisotropic coupling arises in the laboratory frame while in the comoving frame all interactions are reciprocal. Hence, from Eqs. (5) and (6), we can write the constitutive equations of the space–time-modulated media in the comoving frame as

$$\begin{bmatrix}\mathbf{D}'\\ \mathbf{B}'\end{bmatrix} = \begin{bmatrix}\hat{\boldsymbol{\epsilon}}' & \hat{\boldsymbol{\xi}}'\\ \hat{\boldsymbol{\zeta}}' & \hat{\boldsymbol{\mu}}'\end{bmatrix}\begin{bmatrix}\mathbf{E}'\\ \mathbf{H}'\end{bmatrix} \tag{7}$$

which represents a uniaxial medium,

$$\hat{\boldsymbol{\epsilon}}' = \begin{bmatrix}\epsilon'_{||} & 0 & 0\\ 0 & \epsilon'_{\perp} & 0\\ 0 & 0 & \epsilon'_{\perp}\end{bmatrix}, \hat{\boldsymbol{\mu}}' = \begin{bmatrix}\mu'_{||} & 0 & 0\\ 0 & \mu'_{\perp} & 0\\ 0 & 0 & \mu'_{\perp}\end{bmatrix}, \tag{8}$$

with a nonreciprocal magnetoelectric coupling $\hat{\boldsymbol{\zeta}}' = -\hat{\boldsymbol{\xi}}'$, and

$$\hat{\boldsymbol{\xi}}' = \begin{bmatrix}0 & 0 & 0\\ 0 & 0 & -\xi'\\ 0 & +\xi' & 0\end{bmatrix}, \tag{9}$$

where each component reads

$$\epsilon'_{||}(x') = \epsilon(x'), \tag{10}$$

$$\mu'_{||}(x') = \mu(x'), \tag{11}$$

$$\epsilon'_{\perp}(x') = \frac{\epsilon(x')}{1-\epsilon(x')\mu(x')v^2}, \tag{12}$$

$$\mu'_{\perp}(x') = \frac{\mu(x')}{1-\epsilon(x')\mu(x')v^2}, \tag{13}$$

$$\xi'(x') = -v\frac{\epsilon(x')\mu(x')}{1-\epsilon(x')\mu(x')v^2}. \tag{14}$$

In this frame, all the quantities in the constitutive matrix depend solely on x', so we can write the effective parameters by homogenizing over the unit cell following the conventional procedure. This is in contrast to Maxwell's equations in the laboratory frame, where the material parameters depend on both space and time and conventional homogenization cannot be performed.

We stress that we make use of a Galilean transformation and as a consequence this approach is valid for other wave theories. This is suited for this problem because we are dealing with modulated and not moving media. In the Supplemental Material [32], we show how the Galilean transformation of the electromagnetic problem is derived as a standard limiting case of Lorentz transformations.

III. HOMOGENIZATION

We now homogenize the material parameters in the comoving frame. From the continuity of the normal components of $\mathbf{D}$ and $\mathbf{B}$ at an interface, we have that in the long-wavelength limit, $\langle\mathbf{D}'_{||}\rangle = \mathbf{D}'_{||}$ and $\langle\mathbf{B}'_{||}\rangle = \mathbf{B}'_{||}$. Then, for the parallel components of the fields, we write Eqs. (5) as $\langle\mathbf{D}'_{||}/\epsilon(x')\rangle = \langle\mathbf{E}'_{||}\rangle$ and $\langle\mathbf{B}'_{||}/\mu(x')\rangle = \langle\mathbf{H}'_{||}\rangle$, and we have

$$\langle\mathbf{D}'_{||}\rangle = \left\langle\frac{1}{\epsilon(x')}\right\rangle^{-1}\langle\mathbf{E}'_{||}\rangle, \tag{15}$$

$$\langle\mathbf{B}'_{||}\rangle = \left\langle\frac{1}{\mu(x')}\right\rangle^{-1}\langle\mathbf{H}'_{||}\rangle. \tag{16}$$

Hence, the effective permittivity and permeability in the parallel direction are given by

$$\overline{\epsilon'}_{||} = \left[\frac{1}{d}\int_0^d \frac{1}{\epsilon'_{||}(x')}\,dx'\right]^{-1} \tag{17}$$

$$\overline{\mu'}_{||} = \left[\frac{1}{d}\int_0^d \frac{1}{\mu'_{||}(x')}\,dx'\right]^{-1}, \tag{18}$$

where d is the spatial periodicity of the modulation. On the other hand, from the continuity of the tangential components of $\mathbf{E}$ and $\mathbf{H}$ at an interface, we have that $\langle\mathbf{E}'_{\perp}\rangle = \mathbf{E}'_{\perp}$

and $\langle \mathbf{H}'_\perp \rangle = \mathbf{H}'_\perp$. Hence, for the perpendicular components of the fields, we have, from Eq. (6), $\langle \mathbf{D}'_\perp \rangle = \langle \boldsymbol{\epsilon}_\perp(x')\mathbf{E}' + \boldsymbol{\xi}(x')\mathbf{H}' \rangle$ and $\langle \mathbf{B}'_\perp \rangle = \langle \boldsymbol{\mu}_\perp(x')\mathbf{H}' - \boldsymbol{\xi}(x')\mathbf{E}' \rangle$, and

$$\langle \mathbf{D}'_\perp \rangle = \langle \boldsymbol{\epsilon}_\perp(x') \rangle \langle \mathbf{E}'_\perp \rangle + \langle \boldsymbol{\xi}(x') \rangle \langle \mathbf{H}'_\perp \rangle, \tag{19}$$

$$\langle \mathbf{B}'_\perp \rangle = \langle \boldsymbol{\mu}_\perp(x') \rangle \langle \mathbf{H}'_\perp \rangle - \langle \boldsymbol{\xi}(x') \rangle \langle \mathbf{E}'_\perp \rangle. \tag{20}$$

Hence, the remaining effective parameters are given by

$$\overline{\epsilon'}_\perp = \frac{1}{d}\int_0^d \epsilon'_\perp(x')\, dx', \tag{21}$$

$$\overline{\mu'}_\perp = \frac{1}{d}\int_0^d \mu'_\perp(x')\, dx', \tag{22}$$

$$\overline{\xi'} = \frac{1}{d}\int_0^d \xi'(x')\, dx'. \tag{23}$$

Here, we assume that the frequency and momentum of the waves of interest are much smaller than the modulation temporal and spatial frequencies.

The above set of Eqs. (17), (18), and (21)–(23) provide the effective-medium description of space-time modulations of traveling-wave form in the comoving frame. The last step is to transform them to the laboratory frame, where the uniaxial and nonreciprocal structure of the parameters is maintained. The effective-medium parameters in the stationary frame have the same matrix form as in the comoving frame, Eqs. (8)–(9), and

$$\hat{\boldsymbol{\xi}}^{\text{eff}} = \begin{bmatrix} 0 & 0 & 0 \\ 0 & 0 & +\xi^{\text{eff}} \\ 0 & -\xi^{\text{eff}} & 0 \end{bmatrix}, \tag{24}$$

with components given by

$$\epsilon_{||}^{\text{eff}} = \overline{\epsilon'}_{||}, \tag{25}$$

$$\mu_{||}^{\text{eff}} = \overline{\mu'}_{||}, \tag{26}$$

$$\epsilon_\perp^{\text{eff}} = \frac{\overline{\epsilon'}_\perp}{(1-v\overline{\xi'})^2 - v^2\overline{\epsilon'}_\perp\,\overline{\mu'}_\perp}, \tag{27}$$

$$\mu_\perp^{\text{eff}} = \frac{\overline{\mu'}_\perp}{(1-v\overline{\xi'})^2 - v^2\overline{\epsilon'}_\perp\,\overline{\mu'}_\perp}, \tag{28}$$

$$\xi^{\text{eff}} = -\frac{v\overline{\epsilon'}_\perp\,\overline{\mu'}_\perp + (1-v\overline{\xi'})\overline{\xi'}}{(1-v\overline{\xi'})^2 - v^2\overline{\epsilon'}_\perp\,\overline{\mu'}_\perp}. \tag{29}$$

This set of equations, together with Eqs. (17), (18), and (21)–(23), constitute the main result of this paper. They prescribe how to calculate the effective material parameters of any space-time modulation of traveling-wave type. With them, we can write the effective mode dispersion relation as

$$\mu_\perp^{\text{eff}}\epsilon_\perp^{\text{eff}}\omega^2 = \frac{\mu_\perp^{\text{eff}}}{\mu_{||}^{\text{eff}}}k_y^2 + (k - \xi^{\text{eff}}\omega)^2,\ s\text{-polarization}, \tag{30}$$

$$\mu_\perp^{\text{eff}}\epsilon_\perp^{\text{eff}}\omega^2 = \frac{\epsilon_\perp^{\text{eff}}}{\epsilon_{||}^{\text{eff}}}k_y^2 + (k - \xi^{\text{eff}}\omega)^2,\ p\text{-polarization}, \tag{31}$$

Finally, from this, we obtain the effective group velocity of modes co- and counterpropagating with the modulation in terms of the effective parameters as $v_{\text{eff}}^{\pm} = \omega/k^{\pm}$,

$$v_{\text{eff}}^{\pm} = \frac{1}{\pm\sqrt{\epsilon_\perp^{\text{eff}}\mu_\perp^{\text{eff}}} + \xi^{\text{eff}}}, \tag{32}$$

where the $\pm$ sign correspond to forward- and backward-propagating waves, respectively.

Importantly, these formulas show that for any kind of traveling-wave modulations where only one of the parameters is modulated, that is, only the permittivity or only the permeability, then $\xi^{\text{eff}} = 0$ and there is no bianisotropy at long wavelengths. In fact, any synthetic motion implies bianisotropy in the comoving frame, that is, the average, $\overline{\xi'}$, of the magnetoelectric coupling, $\xi'(x')$, is nonzero as long as one parameter is modulated. However, in transforming to the laboratory frame, the effective magnetoelectric coupling, ξ^{eff}, cancels out if only one parameter is modulated (for a detailed proof, see the Supplemental Material [32]) and the effective medium is reciprocal, with $v_{\text{eff}}^{+} = v_{\text{eff}}^{-}$, as expected. Thus, our formalism analytically proves in an exact form that nonreciprocity can be extended beyond the high-frequency band-gap regions [3,7] into the long-wavelength regime under certain conditions [10,12]. This also sheds light on nonreciprocal behaviors observed in other physical systems, such as the asymmetric diffusion of charge based on space-time modulations [13].

IV. CONDITIONS FOR AN EXACT THEORY

We now introduce an exact solution to Maxwell's equations and show that the above effective-medium theory is, in fact, exact under certain conditions. In matched space–time-modulated systems, Maxwell's equations can be solved analytically in the comoving frame. This is seen by noting that with equal modulations of the permittivity and the permeability, the medium impedance is constant,

$$\frac{\mu(x,t)}{\epsilon(x,t)} = Z^2, \tag{33}$$

and we can write

$$E_\perp = \pm\,\sigma_{s,p} Z H_\perp, \quad D_\perp = \pm\,\sigma_{s,p} Z^{-1} B_\perp, \tag{34}$$

where the top (bottom) sign corresponds to forward- (backward-) propagating waves, and $\sigma_s = -1$ for s-polarization ($E_\perp = E_z$), and $\sigma_p = +1$ for p-polarization ($H_\perp = H_z$). At normal incidence, the perpendicular components of Maxwell's equations in the laboratory frame, Eq. (2), read as

$$\sigma_{s,p}\,\partial_x E_\perp = -\partial_t B_\perp, \quad \sigma_{s,p}\,\partial_x H_\perp = -\partial_t D_\perp. \tag{35}$$

Making use of Eqs. (34) and given that the medium impedance is constant, both equations reduce to one (for more details, see the Supplemental Material [32]),

$$\frac{\partial}{\partial x}\left[\epsilon(x,t)^{-1} D_\perp\right] = \mp Z \frac{\partial D_\perp}{\partial t}, \tag{36}$$

with the $-$ and $+$ signs corresponding to forward and backward wave propagation, respectively. By transforming to the Galilean frame comoving with the space-time modulation, as in Sec. II, we arrive at a partial differential equation for $D_\perp$,

$$\frac{\partial}{\partial x'}\left[\left(\pm c(x') - v\right) D_\perp\right] = -\frac{\partial D_\perp}{\partial t'}, \tag{37}$$

where we introduce $c(x') = Z^{-1}\epsilon(x')^{-1}$ as the local wave velocity. In the frequency domain, we have

$$\ln\left[D_\perp\left(\pm c(x') - v\right)\right] = i\omega' \int \frac{1}{\pm c(x') - v} dx', \tag{38}$$

where we can identify a mode wave vector by considering that, given the absence of back reflections, the phase accumulated in one spatial period equals the phase shift of Bloch modes across the unit cell, $\Delta\phi = k_{\text{eff}}^{\pm} d$. Hence, we have

$$k^{\pm} = \omega' \frac{1}{d} \int_0^d \frac{1}{\pm c(x') - v} dx'. \tag{39}$$

When the grating modulation speed is large enough to approach the local velocity of light at any point within the grating, there is a singular point at $c(x') = v$, where the integrand diverges for waves that copropagate with the space-time modulation ($+$ sign in the integrand). As a result, the effective group velocity of forward waves in the comoving frame approaches zero. At this point, in the laboratory frame, the dispersion lines of forward modes of different orders become arbitrarily close and are parallel to the dispersion of waves in the background (unmodulated) medium. This marks the onset of the previously identified *luminal* regime [25], where Bloch theory fails and an effective-medium description of the system is no longer valid [see Fig. 1(c)], although our analytical approach can be further extended to the study of this regime [33]. Additionally, we note that this singularity is related to that emerging in black-hole analog models [34].

Finally, from the dispersion relation of forward- and backward-propagating waves in the comoving frame, $k^{\pm} = \omega(\pm\sqrt{\epsilon'_\perp \mu'_\perp} - \xi')$, we can derive the electromagnetic parameters as

$$\begin{aligned}\epsilon'_\perp = \mu'_\perp &= \sqrt{\epsilon'_\perp \mu'_\perp} = \frac{1}{2\omega}(k^+ - k^-) \\ &= \frac{1}{d}\int_0^d \frac{\epsilon(x')}{1 - \epsilon(x')\mu(x')v^2} dx', \end{aligned} \tag{40}$$

$$\begin{aligned}\xi' &= -\frac{1}{2\omega}(k^+ + k^-) \\ &= -v\frac{1}{d}\int_0^d \frac{\epsilon(x')\mu(x')}{1 - \epsilon(x')\mu(x')v^2} dx', \end{aligned} \tag{41}$$

yielding the same results as the homogenization formulas. This proves that the homogenization theory is, in fact, exact at any frequency in the absence of backscattering, or at sufficiently low frequencies (compared to the modulation frequency) in nonmatched systems, since backscattering is negligible far below the band gaps. In the Supplemental Material [32], we provide an alternative proof based on transfer-matrix theory.

Our homogenization framework as well as the exact theory can be readily applied to any kind of traveling-wave space–time-modulated media. In the following, we unify two different classes of traveling-wave media that are commonly considered, by applying our formulas to the cases of (i) traveling stratified media and (ii) sinusoidal space-time media and deriving their corresponding analytical effective-medium parameters.

V. TRAVELING STRATIFIED MEDIA

Let us consider a traveling two-layer stratified medium with relative parameters (ϵ_1, μ_1) and (ϵ_2, μ_2) and thicknesses d_1 and d_2 (period $d = d_1 + d_2$), modulated at speed v. In this case, the integrals in Eqs. (10)–(23) straightforwardly give the set of effective parameters in the comoving frame,

$$\frac{\overline{\epsilon}'_{||}}{\epsilon_0} = \left(\frac{d_1}{d}\frac{1}{\epsilon_1} + \frac{d_2}{d}\frac{1}{\epsilon_2}\right)^{-1}, \tag{42}$$

$$\frac{\overline{\mu}'_{||}}{\mu_0} = \left(\frac{d_1}{d}\frac{1}{\mu_1} + \frac{d_2}{d}\frac{1}{\mu_2}\right)^{-1}, \tag{43}$$

$$\frac{\overline{\epsilon}'_{\perp}}{\mu_0} = \frac{1}{d}\left(\frac{\epsilon_1}{1 - \epsilon_1\mu_1 v^2/c_0^2} d_1 + \frac{\epsilon_2}{1 - \epsilon_2\mu_2 v^2/c_0^2} d_2\right), \tag{44}$$

$$\frac{\overline{\mu}'_{\perp}}{\mu_0} = \frac{1}{d}\left(\frac{\mu_1}{1-\epsilon_1\mu_1 v^2/c_0^2}d_1 + \frac{\mu_2}{1-\epsilon_2\mu_2 v^2/c_0^2}d_2\right), \tag{45}$$

$$\overline{\xi}' c_0 = -\frac{v}{dc_0}\left(\frac{\epsilon_1\mu_1 d_1}{1-\epsilon_1\mu_1 v^2/c_0^2} + \frac{\epsilon_2\mu_2 d_2}{1-\epsilon_2\mu_2 v^2/c_0^2}\right), \tag{46}$$

which need to be transformed to the rest frame through Eqs. (25)–(29). From the laboratory-frame effective parameters, which are given in the Supplemental Material [32], the effective wave velocity can be obtained through Eq. (32). Alternatively, for matched systems, the effective wave velocity can be derived from the exact Eq. (39) and transformation to the rest frame (see the Supplemental Material [32]).

We now particularize to a traveling bilayer crystal with $\epsilon_{1,2} = \epsilon_m(1 \pm \alpha_e)$, $\mu_{1,2} = \mu_m(1 \pm \alpha_m)$, such that the permittivity and permeability are symmetrically shifted above and below the background values, ϵ_m, μ_m. We first consider the case of matched space-time modulations, with $\alpha_{e,m} = \alpha = 0.1$, constant impedance $Z_1 = Z_2 = Z_0\sqrt{\mu_m/\epsilon_m}$, and $d_1 = d_2$. In this case, the theory is exact and the effective parameters in the rest frame reduce to

$$\frac{\epsilon_{\perp}^{\text{eff}}}{\epsilon_0} = \epsilon_m \frac{1-\left(1-\alpha^2\right)v^2 c_m^{-2}c_0^{-2}}{1-v^2c_m^{-2}c_0^{-2}}, \tag{47}$$

$$\frac{\mu_{\perp}^{\text{eff}}}{\epsilon_0} = \mu_m \frac{1-\left(1-\alpha^2\right)v^2 c_m^{-2}c_0^{-2}}{1-v^2c_m^{-2}c_0^{-2}}, \tag{48}$$

$$\xi^{\text{eff}} c_0 = \alpha^2 \frac{v c_0^{-1} c_m^{-2}}{1-v^2c_m^{-2}c_0^{-2}}. \tag{49}$$

Here, $c_m = 1/\sqrt{\epsilon_m\mu_m}$ is the relative wave velocity in the unmodulated background medium. From the effective parameters, we can obtain the effective wave velocities as

$$v_{\text{eff}}^{\pm} = \pm c_0 c_m \frac{1 \mp v c_m^{-1} c_0^{-1}}{1 \mp v c_m^{-1} c_0^{-1}(1-\alpha^2)}. \tag{50}$$

From the above, we see that if the modulation is only spatial ($v = 0$), $v_{\text{eff}}^{\pm} = \pm c_m c_0$. In fact, this is a particular case of $v_{\text{eff}}^{\pm} = \pm d/(d_1/c_1 + d_2/c_2)$, the conventional homogenization result for space-only stratified media, with $c_1 = 1/\sqrt{\epsilon_1\mu_1}$ and $c_2 = 1/\sqrt{\epsilon_2\mu_2}$ being the relative wave velocities in each of the layers. On the other hand, if the modulation is only temporal ($v \to \infty$), $v_{\text{eff}}^{\pm} \to \pm c_m c_0/(1-\alpha^2)$, which is a particular case of $v_{\text{eff}}^{\pm} = \pm(c_1 d_1 + d_2 c_2)/d$, the average wave velocity for time-only stratified media [35]. Additionally, our results for space-time bilayers are consistent with those derived using a different method [36] but, given that the system is matched, these analytical results give the exact photonic band structure at any frequency. On the other hand, we note that although the effective parameters can be calculated for any modulation speed [except for the pole in Eqs. (47)–(50)], the problem of a traveling stratified medium is ill defined within the speed range limited by the group velocity of waves in each layer, $c_1 < v/c_0 < c_2$. In fact, when the modulation speed equals the group velocity of waves in any of the crystal layers, $v/c_0 = c_{1,2}$, the effective parameters in the comoving frame diverge [see Eqs. (44)–(46)], which results in singularities in the effective parameters that, while being removable, mark the limits of a range of velocities where there are exponentially growing solutions and homogenization is not valid.

The expression for the effective wave velocities, Eq. (50), reveals that away from the space-only or time-only modulations, forward and backward modes are affected very differently by the space-time modulation. Figure 2 shows the relative effective parameters of this system with $\alpha = 0.1$. The effective group velocity in the rest frame, v_{eff}, is shown in panel (a) for the forward (blue, left axis) and backward (orange, right axis) waves, while panel (b) presents the effective permittivity, permeability, and magnetoelectric coupling. The range $c_1 < v/c_0 < c_2$ is marked with a shaded area. At zero modulation speed, forward and backward modes start at $\pm c_m c_0$. As the modulation speed increases, the effective velocity of backward waves changes very little and monotonously up to $-c_m c_0/(1-\alpha^2)$ at $v \to \infty$. In fact, this is a consequence of the back-reflection-free condition: backward waves interact very little with the modulation. On the other hand, forward waves are strongly affected by it. In the subluminal regime, $v < c_1 c_0$, the effective forward wave velocity is smaller than the wave velocity in the background medium, $v_{\text{eff}}^{+} < c_m c_0$, and it decreases as the modulation speed increases. This is consistent with the effective refractive index and the magnetoelectric coupling increasing with modulation speed [see panel (b)]. On the other hand, when the singularity is crossed and the modulation is superluminal, $v > c_2 c_0$, the effective velocity changes from being smaller to being larger than the background wave velocity and then it decreases again up to the limiting value as the modulation speed decreases, consistent with effective parameters smaller than the background parameters and negative magnetoelectric coupling [see panel (b)].

Having considered a matched space-time modulation, we now look at general values of $(\alpha_e, \alpha_m) = \sqrt{2}\alpha(\cos\phi, \sin\phi)$, while keeping all the parameters the same and assuming low frequencies. For $\phi = \pi/4$, we recover the matched case studied above, $\alpha_{e,m} = \alpha$. Specifically, in Fig. 2(c), we show the effective magnetoelectric coupling, ξ^{eff}, as a function of the modulation speed and ϕ, the parametrization angle that determines the values of (α_e, α_m). Shaded in gray is the range of modulation speeds where homogenization is not valid, $c_1 < v/c_0 < c_2$, which is widest when the system is matched ($\alpha_{e,m} = \pm\alpha$) and vanishes to a point when the electric and magnetic modulations are completely out of phase with each other, ($\pm\alpha_e =$

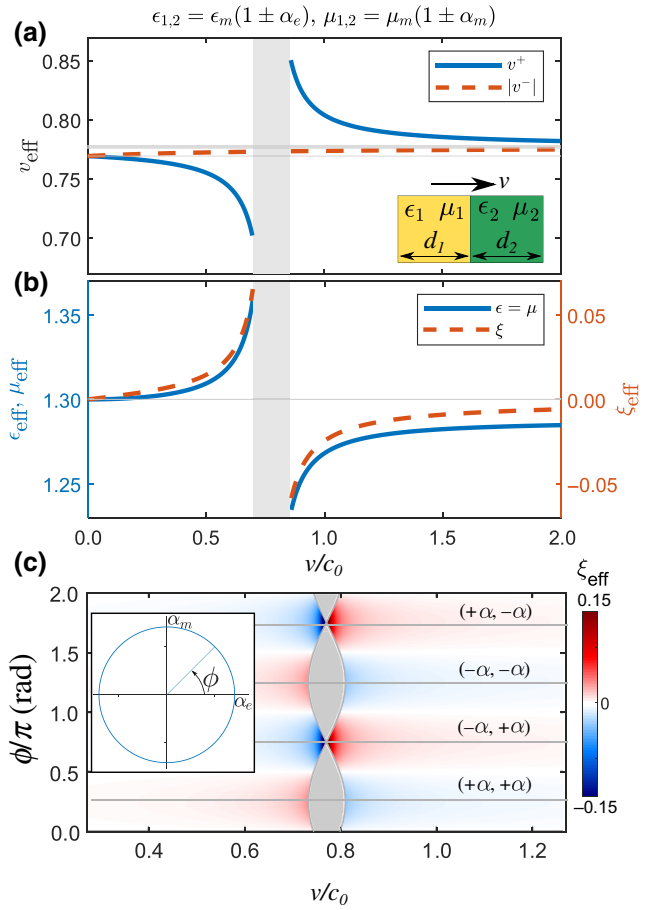

FIG. 2. The group velocity and effective parameters for a traveling bilayered medium as a function of the speed, v. (a) The group velocity, in absolute value, of forward (blue, solid) and backward (orange, dashed) waves, for matched space-time modulations, $\alpha_e = \alpha_m = 0.1$. The range of modulations where a homogenization picture is not valid, $c_1 < v/c_0 < c_2$, is marked with a gray area. (b) The effective permittivity, $\epsilon_\perp^{\rm eff}$, and permeability, $\mu_\perp^{\rm eff}$ (left axis), and the magnetoelectric coupling $\xi_{\rm eff}$ (right axis). (c) The effective magnetoelectric coupling as a function of the space-time modulation speed, v, and the values of (α_e, α_m), parametrized by ϕ, as shown in the inset panel. We take $\epsilon_m = \mu_m = 1.3$ and $d_1 = d_2 = d/2$. We show relative values of the wave velocity and effective parameters, i.e., $v_{\rm eff}$ is in units of c_0, $\epsilon_{\rm eff}$ and $\mu_{\rm eff}$ are in units of ϵ_0 and μ_0, respectively, and $\xi_{\rm eff}$ is in units of c_0^{-1}.

$\mp\alpha_m$). The behavior of $\xi^{\rm eff}$ clearly shows that if only one of the parameters is modulated, that is, if either α_e or α_m are 0 ($\phi = n\pi/2$, $n = 0, 1, \ldots$), the system is reciprocal, since $\xi^{\rm eff} = 0$. Conversely, when $\alpha_e = \pm\alpha_m$ ($\phi = n\pi/4$, $n = 1, \ldots$), nonreciprocity is maximum, as $\xi^{\rm eff}$ is maximum. As ϕ changes and the relative sign between the electrical and magnetic modulations change, $\xi^{\rm eff}$ changes sign. Furthermore, the sign of the effective magnetoelectric coupling changes when the modulation speed goes from sub- ($v < c_1$) to superluminal ($v > c_2$) for any phase between the electric and magnetic modulations. It is interesting to note that when the electric and magnetic modulations are completely out of phase and the region where homogenization is not valid shrinks to a point, the magnetoelectric coupling increases considerably, giving rise to large nonreciprocal effects. The results discussed in this section prove that nonreciprocity can be tuned in space–time-modulated stratified media by changing the modulation speed, or the phase between electric and magnetic modulations.

VI. SINUSOIDAL TRAVELING-WAVE MODULATIONS

We now consider a sinusoidal traveling-wave modulation,

$$\epsilon(x,t) = \epsilon_m\epsilon_0[1 + 2\alpha_e\cos(gx - \Omega t)], \tag{51}$$

$$\mu(x,t) = \mu_m\mu_0[1 + 2\alpha_m\cos(gx - \Omega t)], \tag{52}$$

where g and Ω are the spatial and temporal frequencies, $\alpha_{e,m}$ are the electric and magnetic modulation strengths, and ϵ_m and μ_m are the background relative permittivity and permeability of the medium. The profile moves with a phase velocity of $v = \Omega/g$.

We first consider the case of impedance-matched space-time modulations ($\alpha_{e,m} = \alpha$), where the theory is exact, and we make use of the expression for the effective wave speed in the comoving frame. From Eq. (39), we have, for waves copropagating with the modulation,

$$\frac{1}{\overline{v}'_+} = \frac{g}{2\pi}\int_0^{2\pi/g} \frac{1}{c_m c_0[1 + 2\alpha\cos(gx')]^{-1} - v}dx'$$

$$= -\frac{1}{v} \pm \frac{1}{v\sqrt{(1-4\alpha^2)(v - v_c^+)(v - v_c^-)}}, \tag{53}$$

where we introduce $v_c^\pm = c_m c_0(1 \pm 2\alpha)^{-1}$. These modulation speed values correspond to the two critical points where $1/\sqrt{v - v_c^\pm} \to \infty$ and hence the effective wave velocity in the comoving frame goes to zero. Transforming to the rest frame, $v_{\rm eff}^+ = \overline{v}'_+ + v$, we see that at the critical points the effective wave velocity equals the modulation speed, $v_{\rm eff}^+ = v_c$. In the above expression, $+$ ($-$) corresponds to subluminal (superluminal) modulations, which are bounded by the critical modulation speed values: $v < c_m c_0(1 + 2\alpha)^{-1}$ corresponds to the subluminal regime and $v > c_m c_0(1 - 2\alpha)^{-1}$ to the superluminal one. In fact, these critical points distinguish the onset of the luminal regime, $c_m c_0(1 + 2\alpha)^{-1} < v < c_m c_0(1 - 2\alpha)^{-1}$, where the solution to the integral is imaginary, implying from Eq. (38) that the fields can increase without bound. This is in agreement with the previously identified instability region based on Floquet-Bloch theory for modulations of ϵ only [25] or ϵ and μ [10], where unidirectional amplification is possible [18].

In Fig. 3, we present results for traveling-wave impedance-matched space-time modulations with $\alpha = 0.05$ and $\epsilon_m = \mu_m = 1$. Panel (a) shows the rest frame effective wave velocity, v_{eff}/c_0, as a function of the modulation speed, v/c_0, from the exact expression with a solid line. We also show numerical results from Floquet-Bloch theory with green dots, to confirm the accuracy of the result (for details on this approach, see Ref. [12]), as well as numerical evaluation of the homogenization integrals with black dots. Starting at zero modulation speed, where $v_{\text{eff}}^{+} = c_0$ since $c_m = 1$, the forward-wave effective velocity decreases down to a threshold value $v_{\text{eff}}^{+} = c_m c_0 (1+2\alpha)^{-1} \approx 0.91 c_0$ when the modulation speed reaches the subluminal critical point, $v = c_m c_0 (1+2\alpha)^{-1}$. The decrease in effective wave velocity is accompanied by an increase in effective permittivity and permeability, as well as magnetoelectric coupling. On the other hand, after the luminal region, at the superluminal critical point, $v = c_m c_0 (1-2\alpha)^{-1}$, the forward-wave effective velocity takes a limiting value $v_{\text{eff}}^{+} = c_m c_0 (1-2\alpha)^{-1} \approx 1.11 c_0$ and then decreases as the modulation velocity increases, approaching $v_{\text{eff}}^{+} = c_0 (1+2\alpha^2)$. Differently from the traveling stratified crystal, in this case there is a saturation in the value of the wave group velocity at the lower and upper threshold of the range, where homogenization is not valid.

Figures 3(b) and 3(c) show the effective permittivity and permeability ($\epsilon_{\perp}^{\text{eff}}/\epsilon_0 = \mu_{\perp}^{\text{eff}}/\mu_0$, b) and effective magnetoelectric coupling, ($\xi^{\text{eff}} c_0$, c). The homogenization integrals, which we show are exact for impedance-matched systems, can be solved analytically and we use them to plot the effective parameters with a blue line, comparing also to numerically evaluated integrals (plotted with dots). For the matched case under consideration, our method yields

$$\epsilon_{\perp}^{\text{eff}} = \epsilon_m \epsilon_0 \frac{1}{2 v c_0^{-1} c_m^{-1}} \frac{\Gamma_- \mp \Gamma_+}{\Gamma_- \Gamma_+}, \tag{54}$$

$$\mu_{\perp}^{\text{eff}} = \mu_m \mu_0 \frac{1}{2 v c_0^{-1} c_m^{-1}} \frac{\Gamma_- \mp \Gamma_+}{\Gamma_- \Gamma_+}, \tag{55}$$

$$\xi^{\text{eff}} c_0 = -\frac{1}{2 v c_0^{-1}} \frac{\Gamma_- \mp \Gamma_+ - 2\Gamma_- \Gamma_+}{\Gamma_- \Gamma_+}, \tag{56}$$

where the top (bottom) sign corresponds to subluminal (superluminal) speeds and we introduce the shorthand

$$\Gamma_{\pm} = \frac{c_m c_0}{\sqrt{(1-4\alpha^2)(v \pm v_c^{+})(v \pm v_c^{-})}}. \tag{57}$$

We note that the homogenization integrals can be solved analytically for general α_e and α_m, not only for the matched case, and we give the general expressions in the Supplemental Material [32]. In agreement with the effective wave velocity, the effective permittivity and permeability

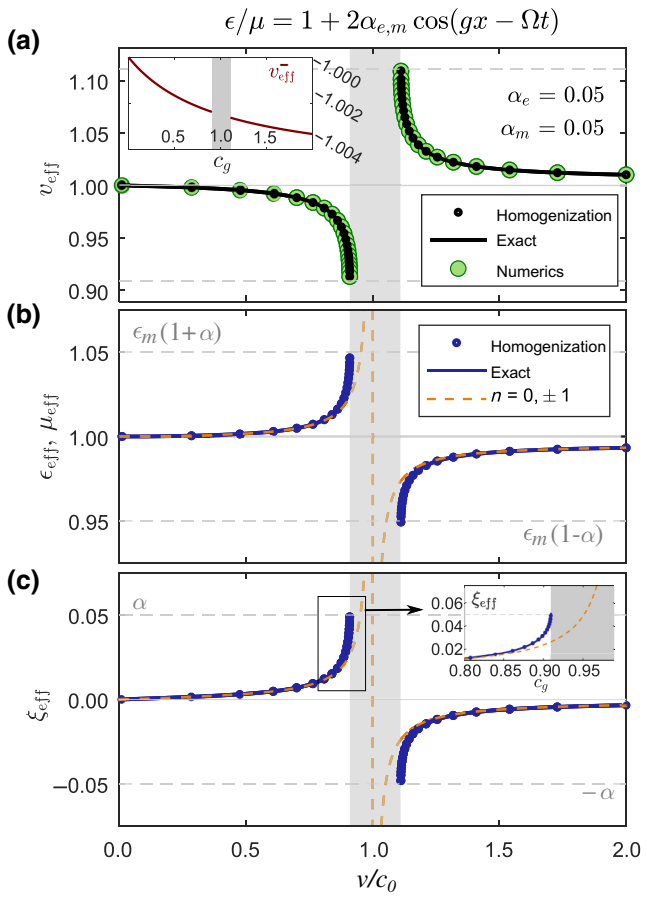

FIG. 3. The group velocity and effective parameters for impedance-matched sinusoidal space-time modulations ($\alpha_e = \alpha_m = 0.05$) as a function of the modulation speed, v. The shaded area represents the unstable regime where a band description loses meaning. (a) The group velocity, v_{eff}, from exact analytical theory (black line), homogenization (black dots), and Floquet-Bloch mode expansion numerics (green circles). (b),(c) The effective permittivity and permeability, $\epsilon_{\perp}^{\text{eff}} = \mu_{\perp}^{\text{eff}}$ (b) and magnetoelectric coupling ξ_{eff} (c). Numerical homogenization (blue dots) and the exact formula (blue line) are compared against a three-mode approximation in the Floquet-Bloch expansion (dashed orange line). In all panels, the limiting values of the effective parameters at the threshold of the luminal regime are depicted with gray dashed horizontal lines. We take $\epsilon_m = \mu_m = 1$. We show relative values of the wave velocity and effective parameters, i.e., v_{eff} is in units of c_0, ϵ_{eff} and μ_{eff} are in units of ϵ_0 and μ_0, respectively, and ξ_{eff} is in units of c_0^{-1}.

increase above the background value and the magnetoelectric coupling increases above zero, as the modulation speed increases from 0 to the subluminal critical speed, $v = c_m c_0 (1+2\alpha)^{-1}$, where $\epsilon_{\perp}^{\text{eff}}/\epsilon_m\epsilon_0 = \mu_{\perp}^{\text{eff}}/\mu_m\mu_0 = 1+\alpha$, and $\xi^{\text{eff}} c_0 = \alpha$. Then, after the luminal region, the permittivity and permeability are reduced below their background values and the magnetoelectric coupling changes sign. They start at threshold values $\epsilon_{\perp}^{\text{eff}}/\epsilon_m\epsilon_0 = \mu_{\perp}^{\text{eff}}/\mu_m\mu_0 = 1-\alpha$, and $\xi^{\text{eff}} c_0 = -\alpha$ when the modulation speed equals

the superluminal critical velocity, $v = c_m c_0 (1+2\alpha)^{-1}$. As the modulation speed increases, they increase, approaching the limiting values at infinite modulation speed, $\epsilon_\perp^{\text{eff}}/\epsilon_0 \to \epsilon_m(1-2\alpha^2)$, $\mu_\perp^{\text{eff}}/\mu_0 \to \mu_m(1-2\alpha^2)$ and $\xi^{\text{eff}} \to 0$. In addition, panels (b) and (c) also show results for the effective parameters (dashed orange line) obtained from a perturbative approach that includes three modes in a Floquet-Bloch expansion. We can see in the plot how this perturbative result is accurate for high and low modulation speeds, as this is a good approximation for small modulation strengths, $\alpha \ll 1$, and modulation speeds far from the luminal region, $v \ll c_m c_0$ or $v \gg c_m c_0$. However, it completely fails to predict the correct behavior close to the luminal regime and, in particular, it misses the saturation of the effective parameters at the critical modulation speeds. These critical points represent a transition between a system described accurately in a Bloch-wave picture and the amplification regime and represent a fundamental difference between the stratified and the sinusoidal traveling-wave modulations. The physics of the transition between these two regimes through the critical point will be studied elsewhere.

Let us now consider general space-time modulations of the permittivity and permeability. We parametrize the electric and magnetic modulations through $(\alpha_e, \alpha_m) = \sqrt{2}\alpha(\cos\phi, \sin\phi)$ and we take $\alpha = 0.05$, such that when $\phi = \pi/4$, we have $\alpha_{e,m} = \alpha$ as in the previously studied case. Figure 4 shows a contour plot of the effective magnetoelectric coupling as a function of the modulation speed, v/c_0, and the parametrization angle, ϕ, similar to what we show for the traveling stratified medium in Fig. 2. The luminal regime is given by the range of modulation speeds limited by the minimum and maximum local group velocities,

$$\frac{c_m}{\sqrt{(1+2\alpha_e)(1+2\alpha_m)}} \le \frac{v}{c_0} \le \frac{c_m}{\sqrt{(1-2\alpha_e)(1-2\alpha_m)}}. \tag{58}$$

This range, which corresponds to the shaded gray area in Fig. 4, has previously been identified for the case of ϵ and μ modulations from Floquet-Bloch theory as the region where a band description of the system fails [10], while here it stems from our analytical treatment. Intuitively, the luminal regime can be understood as the range of modulation velocities bounded by the minimum and maximum local phase velocities of the modulation in the comoving frame $\min[c(x')] \le v \le \max[c(x')]$. As can be seen in Fig. 4, this criterion implies that the luminal regime is widest for the matched case studied above, $\alpha_e = \alpha_m = \pm\alpha$, while it is minimum (width of order α^2) when the modulations are of the same size but out of phase $\alpha_e = -\alpha_m = \pm\alpha$ and its size varies between these extreme cases. While an analytical treatment of this regime is also possible [33,37], here we concentrate on parameters outside of the luminal regime, where the system can be represented by effective material parameters, which, as we show, are exact in the low-frequency limit. Looking at the value of ξ_{eff}, it can be seen that it is nonzero only when both α_e and α_m are nonzero. This implies that whenever both the permittivity and permeability are modulated, the system is nonreciprocal at zero frequency [12]. In addition, we see how the effective magnetoelectric coupling is largest in size at the lower and upper thresholds of the luminal regime. In particular, it can reach giant values for electrical and magnetic modulations of the same size, either matched, $(\pm\alpha, \pm\alpha)$ or in antiphase, $(\pm\alpha, \mp\alpha)$, as we explain in more detail below. The sign of ξ_{eff} changes between the subluminal and superluminal regime and also when the relative sign between α_e and α_m changes, revealing the possibility of tuning the nonreciprocity direction by tuning the modulation speed, or the phase between the electric and magnetic modulations. These findings for electromagnetic systems in the long-wavelength limit also support recent experimental results where the direction of the asymmetric charge flow in a space–time-modulated diffusive system has been tuned by changing the phase between the two available modulating parameters in the system [13], similar to tuning the phase between ϵ and μ in our case. Additionally, to complement the study of the magnetoelectric coupling, in the Supplemental Material [32], we present results for all effective parameters for an instance of nonmatched modulation.

Let us now look in more detail at the giant magnetoelectric coupling obtained when the permittivity and permeability are modulated out of phase by looking at the particular case of antisymmetric modulations, $\alpha_e = -\alpha_m$, that is, $\epsilon/\epsilon_0\epsilon_m = 1 + 2\alpha\cos(gx - \Omega y)$ and $\mu/\mu_0\mu_m = 1 - 2\alpha\cos(gx - \Omega y)$. As is clear from Fig. 4(a), modulating the permittivity and permeability in antiphase leads to the largest values of magnetoelectric coupling and, hence, to large nonreciprocal responses. Additionally, the luminal range is the narrowest: it has width α^2, between the critical values of $v_c^- = c_m c_0$ and $v_c^+ = c_m c_0 (1-4\alpha^2)^{1/2}$. For this case, the analytical solution of the homogenization integrals gives

$$\frac{\epsilon_\perp^{\text{eff}}}{\epsilon_m\epsilon_0} = \frac{\mu_\perp^{\text{eff}}}{\mu_m\mu_0} = \frac{c_m c_0}{v_c^+}\sqrt{\frac{v^2-(v_c^+)^2}{v^2-(v_c^-)^2}}, \tag{59}$$

$$\xi^{\text{eff}} c_0 = \frac{1}{v}\left(1 \mp \frac{c_m c_0}{v_c^+}\sqrt{\frac{v^2-(v_c^+)^2}{v^2-(v_c^-)^2}}\right), \tag{60}$$

where the top (bottom) sign corresponds to subluminal (superluminal) speeds. Figure 4(b) shows the effective parameters in a close-up region around the luminal range for $\alpha_e = -\alpha_m = 0.1$. It is clear that not only does the effective magnetoelectric coupling diverge at the subluminal threshold but so do the effective permittivity and

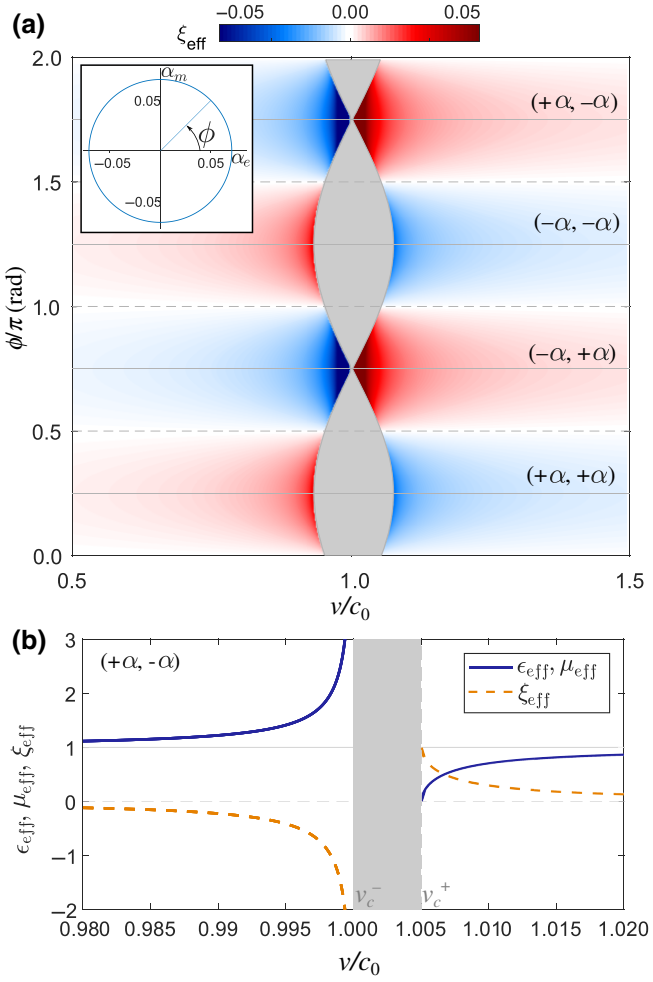

FIG. 4. The effective magnetoelectric coupling for nonmatched systems. (a) ξ_{eff} as a function of the modulation speed, v/c_0, and the values of (α_e, α_m), parametrized by ϕ (see inset). The effective ξ is zero whenever only one of the parameters is modulated (marked with horizontal dashed lines). The gray region centered at $v = c_0$ corresponds to the luminal regime. (b) The effective parameters for antiphased modulations $(+\alpha, -\alpha)$, for a small range close to the luminal regime. The permittivity, $\epsilon_{\text{eff}}/\epsilon_0$, and permeability, μ_{eff}/μ_0, are shown with a solid line and magnetoelectric coupling as a dashed line. We take $\alpha = 0.05$, $\epsilon_m = \mu_m = 1$, and $c_m = 1$, as in Fig. 3. We use units of c_0^{-1} for ξ_{eff}.

permeability. This can be seen from Eqs. (59) and (60), as all the parameters present a divergence as $v \to v_c^-$. On the other hand, at the superluminal threshold, the magnetoelectric coupling saturates, $\xi^{\text{eff}} c_0 \to 1/v_c^+ \sim 1 + 2\alpha^2$, while the permittivity and permeability tend to zero. These results are complemented by the effective mode velocities, which we give in the Supplemental Material [32]. It is curious to note that due to the space-time modulation, and different from standard passive materials, the effective permittivity and permeability can be near zero in the static limit. This analysis explains the origin of the huge magnetoelectric couplings that appear for antiphase modulations of permittivity and permeability.

Finally, we make a connection to the Fresnel drag of light, by establishing an exact mapping between the bianisotropic metamaterial and an equivalent (nonbianisotropic) moving medium. In a previous work, we argue that these metamaterials mimic the relativistic Fresnel-Fizeau drag of light with synthetic motion [12] and without the need for any material motion, in contrast to moving media or metamaterials [38]. Through a perturbative approach, in Ref. [12] we derive effective bianisotropic parameters, accurate for small modulation strengths and low modulation speeds. Here, we employ the framework developed in this work to derive the exact metamaterial parameters and give an exact formula for the Fresnel drag of light in space–time-modulated metamaterials. The nonreciprocal dispersion curves of space-time modulations of both the electric and magnetic parameters can be linked to the relativistic dragging of light by moving matter even though there is no physical motion. In particular, the effective bianisotropic medium characterized by the parameters given in Eqs. (24)–(28) can be mapped to a uniaxial medium with permittivity and permeability tensors,

$$\boldsymbol{\epsilon}_{\text{eq}} = \begin{bmatrix} \epsilon_{\text{eq},||} & 0 & 0 \\ 0 & \epsilon_{\text{eq},\perp} & 0 \\ 0 & 0 & \epsilon_{\text{eq},\perp} \end{bmatrix}, \tag{61}$$

$$\boldsymbol{\mu}_{\text{eq}} = \begin{bmatrix} \mu_{\text{eq},||} & 0 & 0 \\ 0 & \mu_{\text{eq},\perp} & 0 \\ 0 & 0 & \mu_{\text{eq},\perp} \end{bmatrix}, \tag{62}$$

moving with velocity v_D. From a Lorentz transformation between the two frames, we have

$$\epsilon_\perp^{\text{eff}} = \epsilon_{\text{eq},\perp} \frac{1 - v_D^2/c_0^2}{1 - \epsilon_{\text{eq},\perp}^2 \mu_\perp^{\text{eff}} v_D^2/\epsilon_\perp^{\text{eff}}} \tag{63}$$

$$\xi^{\text{eff}} = \frac{v_D}{c_0^2} \frac{\epsilon_\perp'^2 \mu_\perp^{\text{eff}}/\epsilon_\perp^{\text{eff}} c_0^2 - 1}{1 - \epsilon_{\text{eq},\perp}^2 \mu_\perp^{\text{eff}} v_D^2/\epsilon_\perp^{\text{eff}}}, \tag{64}$$

together with $\mu_{\text{eq},\perp} = \epsilon_{\text{eq},\perp} \mu_\perp^{\text{eff}}/\epsilon_\perp^{\text{eff}}$ and $\epsilon_{\text{eq},||} = \epsilon_{||}^{\text{eff}}$, $\mu_{\text{eq},||} = \mu_{||}^{\text{eff}}$. We can then solve the above system for v_D, $\epsilon_{\text{eq},\perp}$ and $\mu_{\text{eq},\perp}$, thus completely characterizing the equivalent moving medium. The obtained analytical expressions are given in the Supplemental Material [32].

Figure 5 shows the equivalent moving-medium parameters and velocity for a space–time-modulated system with parameters $\epsilon_m = \mu_m = 1.3$, $\alpha_e = \alpha_m = 0.05$. For this impedance matched case, we can exploit the exact effective parameters to derive an exact mapping to an equivalent moving medium, shown as blue lines. We also plot with dashed orange lines results obtained from a Floquet-Bloch expansion, assuming three modes for comparison

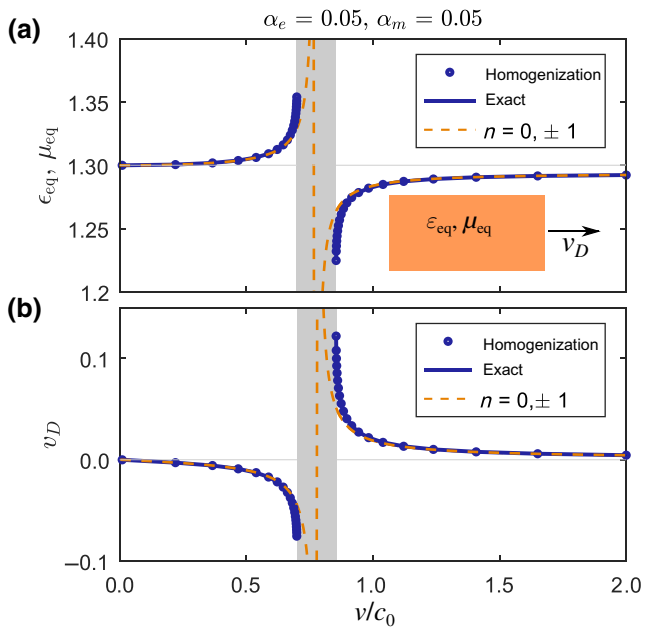

FIG. 5. The electromagnetic parameters, (a) the permittivity and permeability and (b) the velocity, v_D, of the equivalent uniaxial moving medium as a function of the speed modulation. Numerical homogenization (blue dots) and the exact formula (blue line) are compared against a three-mode approximation in the Floquet-Bloch expansion (dashed orange line). We take $\epsilon_m = \mu_m = 1.3$ and $\alpha_e = \alpha_m = 0.05$. The permittivity and permeability are given in units of ϵ_0 and μ_0, respectively, and the drag velocity in units of c_0.

[12]. Similar to the behavior of the effective parameters, the equivalent moving-medium (a) permittivity and permeability and (b) velocity are only defined outside of the luminal range (shaded area). As seen in the plot, the perturbative Floquet-Bloch expansion gives a good approximation for the equivalent moving-medium parameters either at low or very high modulation speeds but it completely fails to predict the correct behavior close to or at luminal speeds. Starting at zero modulation velocity, the equivalent medium is isotropic and stationary, and as the modulation speed increases, the equivalent medium effective parameters increase above the background values, up to a threshold value at the critical subluminal speed that the perturbation theory approach fails to capture (dashed orange line). The equivalent medium velocity is negative and also increases in size down to a threshold value. On the other hand, after crossing the luminal range, the equivalent medium parameters flip to a threshold value below the background parameters at the superluminal critical speed and then approach the background parameters as the modulation speed increases. The velocity of the equivalent moving medium turns positive and decreases toward zero as the modulation approaches a temporal-only modulation. Thus, the drag direction can be switched by switching between sub- and superluminal modulation speeds, while keeping the same modulation direction. The different sign of the drag velocity is linked to the opposite signs of the effective magnetoelectric coupling for sub- and superluminal modulations. In brief, subluminal (superluminal) gratings slow down (speed up) forward waves traveling through the modulated medium and result in equifrequency contours displaced in the same (opposite) direction as the modulation phase velocity [12]. These exact results prove the link between the Fresnel drag of light in moving matter and space–time-modulated media, where there is no physical motion.

Finally, it is worth stressing the different equivalences that we show in this paper. (i) Initially, we consider an isotropic medium subject to a spatiotemporal modulation of its permittivity and permeability. (ii) Through a Galilean transformation, the space-time metamaterial maps to a bianisotropic medium in a frame comoving with the modulation at speed v [Eqs.(21)–(23)]. (iii) In the rest frame, the spatiotemporal metamaterial maps to a bianisotropic effective medium [Eqs. (24)–(28)]. (iv) A Lorentz frame moving at velocity v_D with respect to the laboratory frame can be found where the medium is uniaxial (nonbianisotropic), giving rise to the explanation of the emerging bianisotropy as a Fresnel drag effect.

VII. CONCLUSIONS

To summarize, here we present a complete homogenization framework of space-time metamaterials. While the theory of homogenization has been a cornerstone of the development of the metamaterials field, it has not yet been applied to illuminate the behavior of space-time metamaterials. Additionally, we show that the homogenization approach is exact at low frequencies for general modulations and exact at any frequency in the absence of backscattering, that is, in the case of impedance-matched modulations. Thus, our theory provides analytical expressions for the effective-medium parameters of traveling space-time modulations, which are exact in many practical cases. The theory applies to systems where the modulation frequency is larger than the operating frequency. This regime of operation is more accessible at microwave frequencies, where the assumption of nondispersive media holds and where both the permittivity and permeability can be tuned [12]. As an outlook, including dispersion in the framework will allow us to give accurate predictions of the effective-medium parameters in many temporally modulated systems that are currently being implemented in nanophotonics using graphene, conductive transparent oxides, or ferrites, with higher modulation frequencies currently being achieved in experiments. While we consider the spatiotemporal modulation of an isotropic medium along one dimension, the theory can be extended to more complex scenarios, such as the space-time modulation of nonisotropic media, as well as into more dimensions, and

can shed light on topological transitions or exceptional points that may emerge there. In addition, beyond our focus here on Maxwell's equations, the framework can be extended to other wave theories.

We look in detail at two instances of traveling space-time media: a stratified crystal and a sinusoidal grating. These constitute the two extreme cases of traveling modulations with infinite and a single Fourier component and while they yield similar phenomenology at low and high modulation speeds, we demonstrate that there are differences in their behavior at sub- and superluminal velocities that are close to the instability regime. In the stratified crystal, the effective-medium parameters can, in principle, be calculated within the luminal range where there are no stable solutions, leading to a smooth transition between the homogenized and unstable regimes. On the other hand, in the case of sinusoidal modulations the effective-medium parameters saturate or diverge at the edges of the luminal regime. We expect this critical behavior to lead to rich physics in traveling-wave space–time-modulated metamaterials. Furthermore, our analysis proves that space-time media based on traveling-wave modulations are exactly equivalent (outside the luminal range) to a moving uniaxial uniform material in the long-wavelength regime, with an equivalent velocity of motion that is not the same as the metamaterial modulation speed. Finally, we show how synthetic motion results in giant bianisotropy and hence provides an appealing approach to nonreciprocal metamaterials.

ACKNOWLEDGMENTS

P.A.H. and M.S. acknowledge funding from Fundação para a Ciência e a Tecnologia and Instituto de Telecomunicações under Project No. UIDB/50008/2020. P.A.H. is supported by the CEEC Individual program from Fundação para a Ciência e a Tecnologia with Reference No. CEECIND/02947/2020. E.G. acknowledges support from the Engineering and Physical Sciences Research Council (ESPRC) through the Centre for Doctoral Training in Theory and Simulation of Materials (Grant No. EP/L015579/1) and an EPSRC Doctoral Prize Fellowship (Grant No. EP/T51780X/1). J.B.P. acknowledges funding from the Gordon and Betty Moore Foundation. M.S. also acknowledges support by the IET under the A F Harvey Engineering Research Prize, by the Simons Foundation under the Grant No. 733700 (Simons Collaboration in Mathematics and Physics, "Harnessing Universal Symmetry Concepts for Extreme Wave Phenomena").

[1] A. M. Shaltout, V. M. Shalaev, and M. L. Brongersma, Spatiotemporal light control with active metasurfaces, Science **364**, eaat3100 (2019).

[2] M. Z. Alam, S. A. Schulz, J. Upham, I. De Leon, and R. W. Boyd, Large optical nonlinearity of nanoantennas coupled to an epsilon-near-zero material, Nat. Photonics **12**, 79 (2018).

[3] H. Lira, Z. Yu, S. Fan, and M. Lipson, Electrically Driven Nonreciprocity Induced by Interband Photonic Transition on a Silicon Chip, Phys. Rev. Lett. **109**, 033901 (2012).

[4] C. Caloz and Z. Deck-Léger, Spacetime metamaterials—part I: General concepts, IEEE Trans. Antennas Propagation **68**, 1569 (2020).

[5] J. N. Winn, S. Fan, J. D. Joannopoulos, and E. P. Ippen, Interband transitions in photonic crystals, Phys. Rev. B **59**, 1551 (1999).

[6] F. Biancalana, A. Amann, A. V. Uskov, and E. P. O'reilly, Dynamics of light propagation in spatiotemporal dielectric structures, Phys. Rev. E **75**, 046607 (2007).

[7] Z. Yu and S. Fan, Complete optical isolation created by indirect interband photonic transitions, Nat. Photonics **3**, 91 (2009).

[8] D. L. Sounas and A. Alù, Non-reciprocal photonics based on time modulation, Nat. Photonics **11**, 774 (2017).

[9] Y. Hadad, J. C. Soric, and A. Alu, Breaking temporal symmetries for emission and absorption, Proc. Natl. Acad. Sci. **113**, 3471 (2016).

[10] S. Taravati, Giant Linear Nonreciprocity, Zero Reflection, and Zero Band gap in Equilibrated Space-Time-Varying Media, Phys. Rev. Appl. **9**, 064012 (2018).

[11] D. Torrent, O. Poncelet, and J.-C. Batsale, Nonreciprocal Thermal Material by Spatiotemporal Modulation, Phys. Rev. Lett. **120**, 125501 (2018).

[12] P. A. Huidobro, E. Galiffi, S. Guenneau, R. V. Craster, and J. B. Pendry, Fresnel drag in space–time-modulated metamaterials, Proc. Natl. Acad. Sci. **116**, 24943 (2019).

[13] M. Camacho, B. Edwards, and N. Engheta, Achieving asymmetry and trapping in diffusion with spatiotemporal metamaterials, Nat. Commun. **11**, 3733 (2020).

[14] D.-W. Wang, H.-T. Zhou, M.-J. Guo, J.-X. Zhang, J. Evers, and S.-Y. Zhu, Optical Diode Made from a Moving Photonic Crystal, Phys. Rev. Lett. **110**, 093901 (2013).

[15] D. L. Sounas, C. Caloz, and A. Alu, Giant non-reciprocity at the subwavelength scale using angular momentum-biased metamaterials, Nat. Commun. **4**, 2407 (2013).

[16] K. Fang, Z. Yu, and S. Fan, Photonic Aharonov-Bohm Effect Based on Dynamic Modulation, Phys. Rev. Lett. **108**, 153901 (2012).

[17] N. Chamanara, D. G. Cooke, and C. Caloz, in *2019 IEEE International Symposium on Antennas and Propagation and USNC-URSI Radio Science Meeting* (Atlanta, GA, 2019), p. 239.

[18] E. Galiffi, P. A. Huidobro, and J. B. Pendry, Broadband Nonreciprocal Amplification in Luminal Metamaterials, Phys. Rev. Lett. **123**, 206101 (2019).

[19] Q. Lin, M. Xiao, L. Yuan, and S. Fan, Photonic Weyl point in a two-dimensional resonator lattice with a synthetic frequency dimension, Nat. Commun. **7**, 13731 (2016).

[20] R. Fleury, A. B. Khanikaev, and A. Alu, Floquet topological insulators for sound, Nat. Commun. **7**, 11744 (2016).

[21] L. He, Z. Addison, J. Jin, E. J. Mele, S. G. Johnson, and B. Zhen, Floquet Chern insulators of light, Nat. Commun. **10**, 4194 (2019).

[22] E. Lustig, Y. Sharabi, and M. Segev, Topological aspects of photonic time crystals, Optica **5**, 1390 (2018).
[23] X. Wang, A. Díaz-Rubio, H. Li, S. A. Tretyakov, and A. Alù, Theory and Design of Multifunctional Space-Time Metasurfaces, Phys. Rev. Appl. **13**, 044040 (2020).
[24] A. Oliner and A. Hessel, Wave propagation in a medium with a progressive sinusoidal disturbance, IRE Trans. Microw. Theory Tech. **9**, 337 (1961).
[25] E. Cassedy and A. Oliner, Dispersion relations in time-space periodic media: Part I—Stable interactions, Proc. IEEE **51**, 1342 (1963).
[26] E. Cassedy, Dispersion relations in time-space periodic media part II—Unstable interactions, Proc. IEEE **55**, 1154 (1967).
[27] J. Li, X. Zhu, C. Shen, X. Peng, and S. A. Cummer, Transfer matrix method for the analysis of space-time-modulated media and systems, Phys. Rev. B **100**, 144311 (2019).
[28] S. Taravati, N. Chamanara, and C. Caloz, Nonreciprocal electromagnetic scattering from a periodically space-time modulated slab and application to a quasisonic isolator, Phys. Rev. B **96**, 165144 (2017).
[29] H. T. To, Homogenization of dynamic laminates, J. Math. Anal. Appl. **354**, 518 (2009).
[30] K. Lurie, *An Introduction to the Mathematical Theory of Waves* (Springer, New York, 2007).
[31] H. Nassar, X. Xu, A. Norris, and G. Huang, Modulated phononic crystals: Non-reciprocal wave propagation and Willis materials, J. Mech. Phys. Solids **101**, 10 (2017).
[32] For detailed derivations, see the Supplemental Material at https://link.aps.org/supplemental/10.1103/PhysRevApplied.16.014044, which includes Ref. [39].
[33] J. B. Pendry, E. Galiffi, and P. A. Huidobro, Gain mechanism in time-dependent media, Optica **8**, 636 (2021).
[34] S. J. Robertson, The theory of Hawking radiation in laboratory analogues, J. Phys. B: At. Mol. Opt. Phys. **45**, 163001 (2012).
[35] V. Pacheco-Peña and N. Engheta, Effective medium concept in temporal metamaterials, Nanophotonics **9**, 379 (2020).
[36] Z.-L. Deck-Léger, N. Chamanara, M. Skorobogatiy, M. G. Silveirinha, and C. Caloz, Uniform-velocity spacetime crystals, Advanced Photonics **1**, 1 (2019).
[37] J. B. Pendry, P. A. Huidobro, and E. Galiffi, A new mechanism for gain in time dependent media, arXiv:2009.12077 (2020).
[38] J. C. Halimeh and R. T. Thompson, Fresnel-Fizeau drag: Invisibility conditions for all inertial observers, Phys. Rev. A **93**, 033819 (2016).
[39] J. A. Kong, *Electromagnetic Wave Theory* (Wiley-Interscience, New York, 1986).